

# GEMINI near-infrared spectroscopic observations of young massive stars embedded in molecular clouds

A. Roman-Lopes<sup>1</sup>

<sup>1</sup>*Physics Department - Universidad de La Serena - Cisternas, 1200 - La Serena - Chile*  
roman@dfuls.cl

Z. Abraham<sup>2</sup>

<sup>2</sup>*Departamento de Astronomia, IAG/USP, Rua do Matão, 1226, Cidade Universitária, 05508-900, São Paulo, SP, Brazil*

R. Ortiz<sup>3,2</sup>

<sup>3</sup>*Escola de Artes, Ciências e Humanidades, USP, Av. Arlindo Bettio, 1000, 03828-000, São Paulo, SP, Brazil*

<sup>2</sup>*Departamento de Astronomia, IAG/USP, Rua do Matão, 1226, Cidade Universitária, 05508-900, São Paulo, SP, Brazil*

A. Rodriguez-Ardila<sup>4</sup>

<sup>4</sup>*Laboratório Nacional de Astrofísica, Rua Estados Unidos, 154, Itajubá, 37504-364, Brazil*

## ABSTRACT

*K*-band spectra of young stellar candidates in four southern hemisphere clusters have been obtained with the near-infrared spectrograph GNIRS in Gemini South. The clusters are associated with IRAS sources that have colors characteristic of ultracompact HII regions: IRAS09149-4743, IRAS15408-5356, IRAS16132-5039 and IRAS16177-5018. Spectral types were obtained by comparison of the observed spectra with those of a NIR library; the results include the spectral classification of nine massive stars and seven objects confirmed as background late-type stars. One young stellar object (YSO) was found in each cluster, associated with either the main IRAS source or a nearby resolved MSX component. The distances to the stars were derived from their spectral types and previously determined *JHK* magnitudes; they agree well with previously determined kinematic distances, except in the case of IRAS15408-5356, for which the spectroscopic distance is about a factor two smaller than the kinematic value.

*Subject headings:* stars: early type – stars: fundamental parameters – ISM: Interstellar medium: compact HII regions – near-infrared: young massive stars

## 1. Introduction

Young massive stars are commonly found embedded in high-density molecular clouds. They can be traced, for example, by the presence of CS and NH<sub>3</sub> rotational transitions in the radio spectra of the clouds, and are often associated with

methanol and water masers. The IRAS colours constitute another tool to identify them: Wood & Churchwell (1989) showed that massive stars embedded in dark clouds have steep spectral energy distribution in the infrared, typical of ultracompact HII regions. Therefore, the presence of young massive clusters can be inferred from sur-

veys of radio molecular lines associated with IRAS sources selected according to specific color criteria (Bronfman, Nyman & May 1996); the presence of continuum radio emission and recombination lines toward them confirms that most of these regions are in fact photoionized (Caswell & Haynes 1987). However, these clusters are often affected by high visual extinction, sometimes over 30 magnitudes, which make them undetectable at optical wavelengths, while in the *K*-band for example, the extinction is about a tenth of that in the *V*-band.

Dutra et al. (2003) identified many previously unknown stellar cluster candidates in the 2MASS survey; 2MASS images have been used not only to discover new young clusters, but also to obtain physical properties of their members (Borissova et al. 2003, Leistra et al. 2005). However, its limited spatial resolution ( $\sim 2''$ ) restricts its usage to non-crowded regions, and several authors have taken advantage of the higher spatial resolution provided by a new generation of near-infrared (NIR) array detectors to study clusters with high stellar surface density (Horner, Lada & Lada 1997, Gomes & Kenyon 2001, Hanson, Luhman & Lieke 2002, Massi, Lorenzetti & Giannini 2003, Balog et al. 2004, Kumar, Kamath & Davis 2004, Lada & Muench 2004, Whitney et al. 2004, Figuerêdo et al. 2002, 2005, Arias, Barba & Morrell 2007, Barba & Arias 2007).

Roman-Lopes, Abraham & Lépine (2003); Roman-Lopes & Abraham (2004a,b), Roman-Lopes & Abraham (2006a,b), Ortiz, Roman-Lopes & Abraham (2007), used the NIR camera CamIV, attached to the telescopes at the Pico dos Dias Observatory to study clusters associated to high density molecular clouds, with IRAS colors of ultracompact HII regions. In these studies, *JHK* colour-colour (C-C) and colour-magnitude (C-M) diagrams were used to select the cluster members and estimate their spectral types, since their knowledge is important to determine the initial mass function and to understand the process of cloud fragmentation and star formation. In their work, for each selected star, the corresponding dereddening vector in the C-M diagram was drawn up to the point where it intercepts the ZAMS line. This method depends on an accurate knowledge of at least three parameters: (1) the distance to the cluster; (2) the extinction law in that direction, and (3) the excess

emission due to the possible presence of circumstellar material around each individual star, which affects mainly the *K*-band magnitude.

Most studies of embedded clusters assume kinematic or statistical distances and make use of a standard interstellar extinction law (Rieke & Lebofsky 1985), even though deviations have been reported in dense molecular clouds (Tapia 1981, Indebetouw et al. 2005, Nishyama et al. 2006). In addition to that, it is well established that massive young stellar objects (YSOs) present large infrared excess due to the presence of warm circumstellar dust (Grasdalen et al. 1975, Lada & Adams 1992), which will be reflected in an incorrect estimation of their spectral types. To circumvent part of these problems, spectral types of some of the cluster members can be determined from *K*-band spectroscopy and used to determine the distances to the clusters assuming different extinction laws.

In this work, we present *K*-band spectra of a sample of southern massive star candidates using the Gemini Near Infrared Spectrograph (GNIRS). All targets were selected from previous NIR studies (Roman-Lopes et al. 2003, Roman-Lopes & Abraham 2004a,b, Ortiz et al. 2007). With the present study we intend to determine the true spectral types of the most massive candidates in these clusters, and from them the cluster distances using the spectroscopic parallax technique. Finally, these distances will be compared to those derived from kinematical methods, which eventually can be used to improve the rotation model of our Galaxy.

The paper is organized as follows: Section 2 presents a summary of the four studied regions; Section 3 reports the observations, data reduction and results. In Section 4 we discuss the results obtained for each cluster and in Section 5 we present our conclusions.

## 2. The stellar clusters

The sources chosen for this work belong to young stellar clusters in the southern hemisphere, which are associated with the sources IRAS09149-4743, IRAS15408-5356, IRAS16132-5039 and IRAS16177-5018, previously studied using infrared imaging techniques. In Figure 1 we present NIR images of each cluster (Roman-Lopes et al. 2003, Roman-Lopes & Abraham 2004a,b,

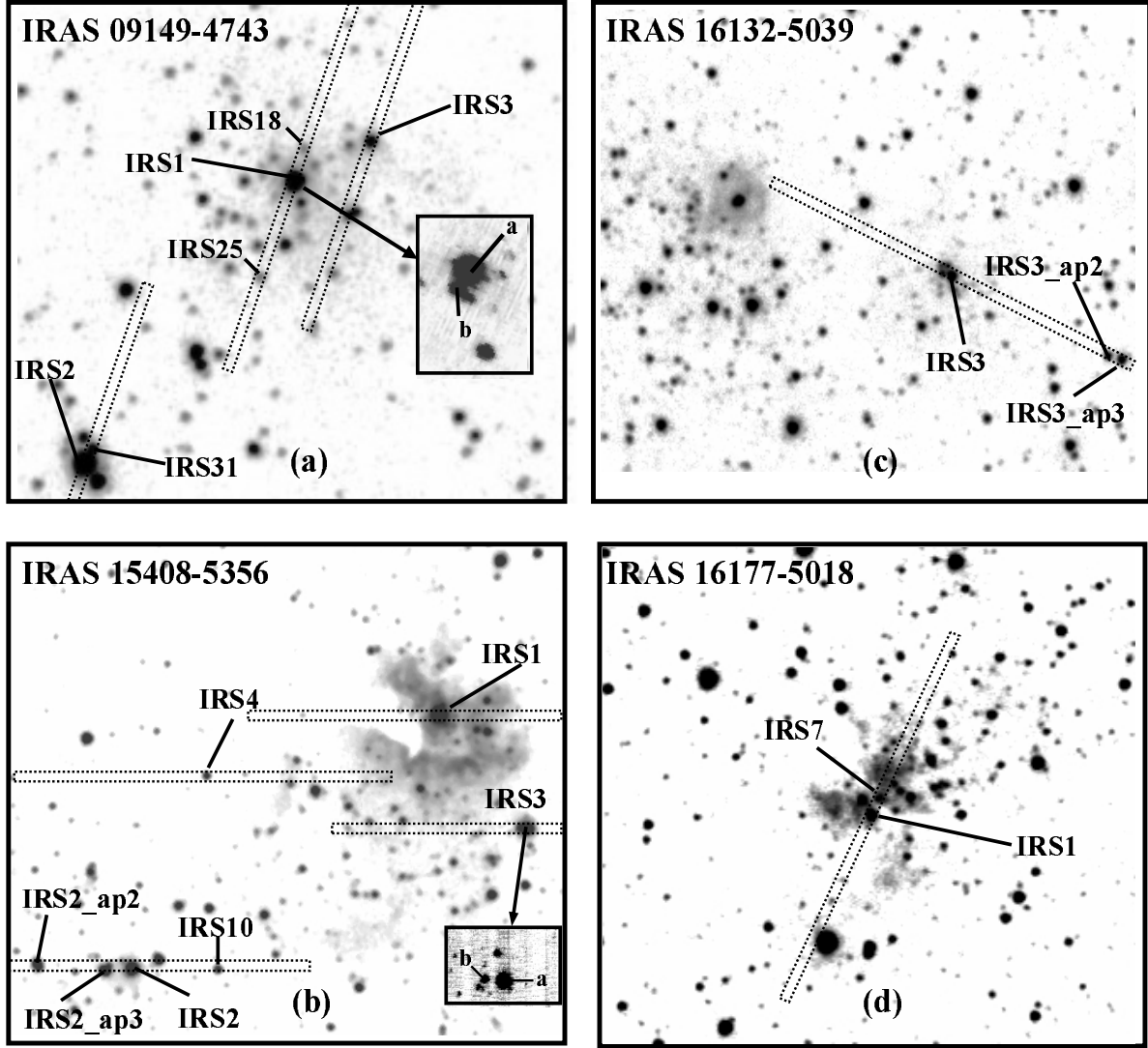


Fig. 1.— NIR finding charts (taken from previous NIR imaging surveys) of the clusters associated to IRAS09149-4743(top-left), IRAS15408-5356(bottom left), IRAS16132-5039(top-right) and IRAS16177-5018(bottom-right) sources. Each image is about  $2' \times 2.5'$  in size. North is to the top, east to the left. In each cluster, we indicate the slit position (dotted lines) and the sources for which we obtained  $K$  band GNIRS spectra. Based on the GNIRS acquisition images, we found that IRAS09149-4743IRS1 and IRAS15408-5356IRS3 are in fact double, as shown in the insets in panels a and b, respectively, at plate scale of  $0.15''$  per pixel.

TABLE 1

LOG-BOOK OF THE GNIRS OBSERVATIONS. THE COLUMNS ARE: (1) THE ASSOCIATED IRAS SOURCE; (2) THE IDENTIFIER OF THE POINT SOURCE, AS DESIGNATED IN THE ORIGINAL PHOTOMETRIC SURVEY; (3,4) EQUATORIAL COORDINATES (J2000.0); (5) THE TOTAL EXPOSURE TIME (s); (6) THE MEAN AIRMASS AT THE TIME OF THE OBSERVATIONS; (7) THE HIPPARCOS IDENTIFIER OF THE ASSOCIATED A0V TELLURIC STAR; (8) THE MEAN AIRMASS OF THE TELLURIC STAR AT THE TIME OF THE OBSERVATIONS; (9) LISTS THE GEMINI IDENTIFICATION PROGRAM AND COLUMN (10) THE CORRESPONDING DATE OF OBSERVATION.

Source (1)	IRS (2)	$\alpha$ (J2000.0) (3)	$\delta$ (J2000.0) (4)	Itime (s) (5)	X (6)	Telluric (7)	X (8)	ID Program (9)	Date (10)
09149-4743	1	09h16m43.50s	-47°56'23.0"	540	1.07	HIP40974	1.03	GS-2005B-Q-33	Dec 23, 2005
09149-4743	2	09h16m47.94s	-47°57'18.0"	132	1.06	HIP40974	1.05	GS-2005B-Q-33	Dec 23, 2005
09149-4743	3	09h16m41.89s	-47°56'15.4"	540	1.05	HIP40974	1.06	GS-2005B-Q-33	Dec 24, 2005
15408-5356	1	15h44m43.40s	-54°05'53.7"	180	1.30	HIP75161	1.36	GS-2005B-Q-33	Dec 24, 2005
15408-5356	2	15h44m43.40s	-54°05'53.7"	180	1.34	HIP75161	1.35	GS-2005B-Q-33	Dec 27, 2005
15408-5356	3	15h44m56.17s	-54°07'18.1"	360	1.57	HIP75161	1.63	GS-2005B-Q-33	Jan 22, 2006
15408-5356	4	15h44m53.04s	-54°06'31.9"	1080	1.64	HIP75161	1.63	GS-2005B-Q-33	Jan 23, 2006
16132-5039	3	16h16m55.99s	-50°47'22.8"	1080	1.88	HIP83406	1.75	GS-2005B-Q-43	Sep 25, 2004
16177-5018	1	16h21m31.60s	-50°25'08.3"	1080	1.56	HIP83818	1.65	GS-2005B-Q-33	Jan 24, 2006

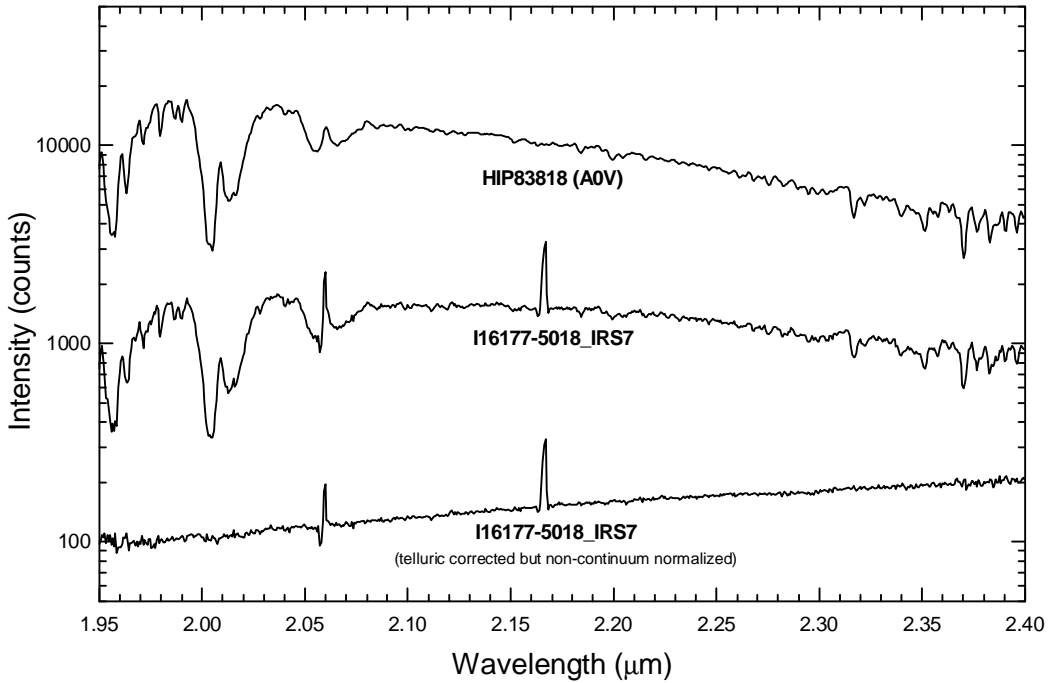


Fig. 2.— Spectra of the A0V standard star HIP83818, the science target IRAS16177-5018 IRS7, and the resulting corrected spectrum (non-continuum normalized)

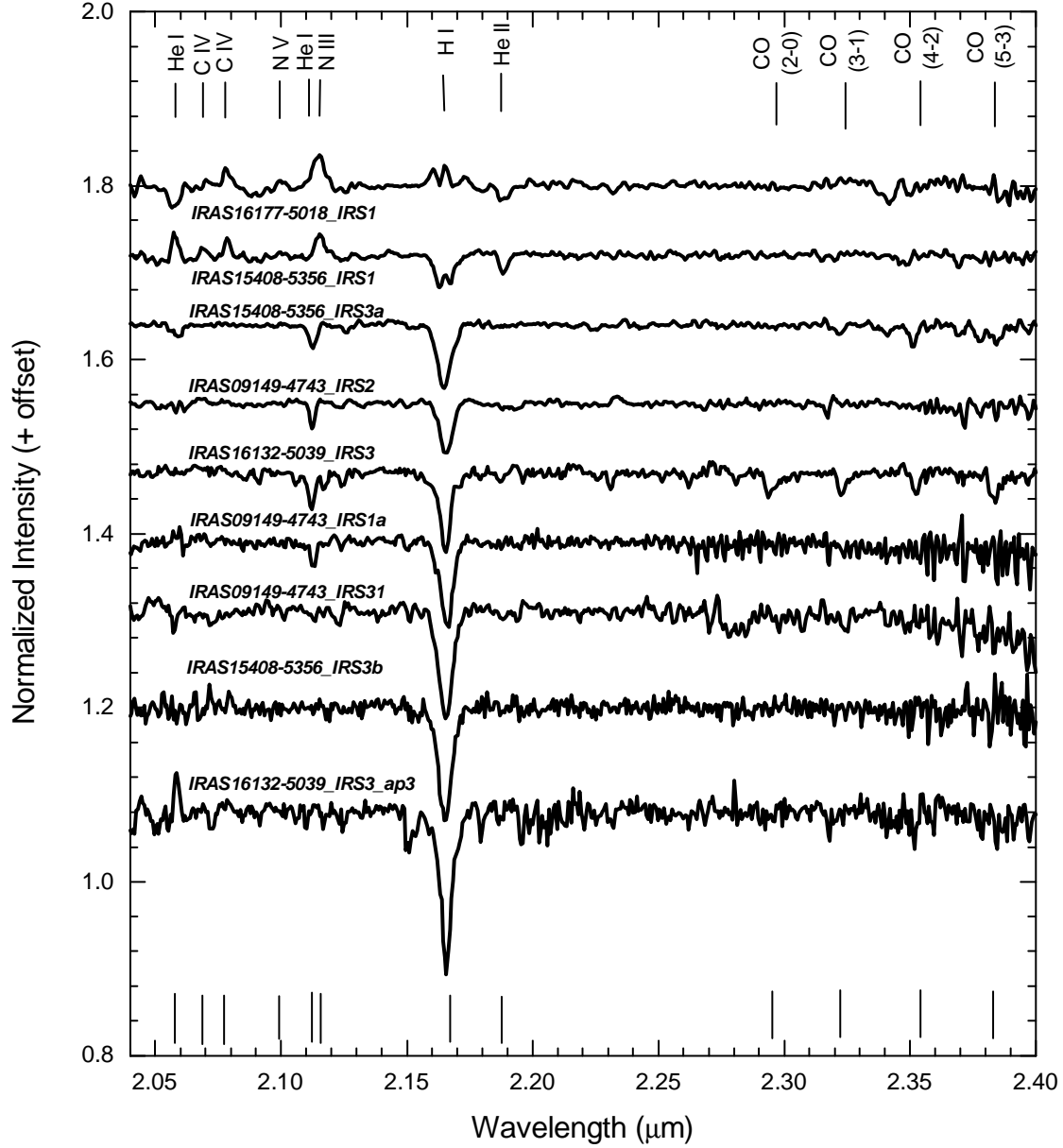


Fig. 3.— GNIRS K-band spectra of the hot stars in our sample. In this figure the GNIRS spectra are flux normalized and are at the same scale.

Ortiz et al. 2007), indicating the position of the observed sources.

The first cluster, associated with IRAS09149-4743, belongs to the Vela Molecular Ridge (VMR), and it is probably related to the optical HII region RCW 41. Ortiz et al.(2007) obtained *JHK* photometry of this cluster at 1.3'' spatial resolution. The authors suggested two stars as the more likely candidates to ionize the nebula: IRS1, located at the centre of the IRAS error ellipse, and IRS2, a member of a small “sub-cluster” containing 6 stars, situated 1.1' southeast of the IRAS position and associated to the MSX6C-G270.2795+00.8353 source. They also found another high-luminosity star in the main cluster, IRS3, which is also the most reddened object in the cluster, suggesting that it might be a background star. A *K*-band image of the region is presented in Figure 1a, where these three program stars are identified, together with other stars that fell into the spectrograph slit and which spectra are also analyzed.

The second cluster is associated with the IRAS source 15408-5356 and the HII region RCW 95; it is seen against a complex galactic structure, the Sagittarius-Carina and Scutum-Crux spiral arms. This cluster was studied in detail by Roman-Lopes & Abraham (2004b), who obtained *JHK* photometry of the region. A nebula is clearly visible in their images, with a clump of embedded stars that include the main ionizing sources of RCW 95, IRS1 and IRS3, as shown in Figure 1b.

The third stellar cluster, shown in Figure 1c, is located towards the IRAS source 16132-5039 and it is associated with the HII region RCW 106. The infrared images obtained by Roman-Lopes & Abraham (2004a) revealed a spheroidal nebula containing a bright star at its centre, IRS1, and a smaller concentration of stars to the south-west of the IRAS source, which coincide with the mid-infrared source MSX5C G332.5302-00.1171; the brightest source in this subcluster is labeled IRS3.

The fourth cluster is associated with IRAS 16177-5018 and, together with IRAS 16132-5039, is embedded in the HII region RCW 106. Roman-Lopes et al. (2003), obtained *JHK* images and photometry of its reddest stars, which have visual extinction exceeding 28 magnitudes. The brightest source is IRS1, located at the centre of the infrared nebula, which together with IRS7, seem to play a key role in the energy balance of the com-

pact HII region (Roman-Lopes et al. 2003). An image of the region, with the two stars indicated, is shown in Figure 1d.

### 3. Observations and results

#### 3.1. GNIRS data

*K*-band spectra for the point sources described in Section 2 were obtained on different dates using GNIRS (Elias et al. 2006) instrument on the 8-m Gemini South telescope at Cerro Pachon, Chile. Table 1 shows the log of observations. In all cases the short camera with a pixel scale of  $0.15'' \text{ pixel}^{-1}$  and a slit size  $0.675'' \times 99''$  was employed. The resolving power of this configuration is 1600, with a wavelength coverage 1.90-2.50 $\mu\text{m}$ . The standard ABBA nodding technique was used to acquire the spectra. Individual exposure time at each nod position was 3 minutes for the science targets; total exposure times are listed in column 5 of Table 1. Before or after the exposure of each target, a nearby A0V spectroscopic standard star was observed at similar airmass (column 7 of Table 1) to remove telluric atmospheric absorption.

The GNIRS data were reduced using the IRAF<sup>1</sup> using sky lines; the typical error ( $1-\sigma$ ) for this calibration was  $\sim 5 \text{ \AA}$ . Multiple exposures for each source were combined, followed by one-dimensional extraction of the spectra. Telluric atmospheric correction using the spectroscopic standard stars completed the reduction process. In this last step, we divided the target spectra by the spectrum of an A0V spectroscopic standard star, already devoided of photospheric features. In this case, the Br $\gamma$  absorption was the only feature present in the *K*-band region. It was carefully removed by interpolation across its wings using continuum points on either side of the line; the core of the line was modeled using a Voigt profile. In order to assure good telluric band cancellation, the IRAF task *telluric* was employed. The algorithm interactively minimizes the RMS in spec-

<sup>1</sup>IRAF is distributed by the National Optical Astronomy Observatories, which are operated by the Association of Universities for Research in Astronomy, INC, under cooperative agreement with the National Science Foundation. Gemini package. First, the 2D *K*-band frames were sky-subtracted for each pair of images taken at the two nod positions A and B, followed by division of the resultant image by a master flat. Thereafter, wavelength calibration was performed

ified wavelength regions by shifting and scaling the target relative to the standard spectrum to best divide out telluric features present in the former. Shifting allows for possible small errors in the dispersion zero-points. Intensity scaling corrects for differences in the airmass and variations in the abundance of the telluric species. It uses Beer's law, which assumes that the absorption varies with abundance through an exponential relationship. Typical values of the shifts were a few tenths of a pixel (equivalent to  $\sim 2 \text{ \AA}$ ) and the scaling factors were not larger than 10%. As an example, in Figure 2 we show the spectra of the A0V standard star HIP83818, the science target IRAS16177-5018\_IRS7, and its corrected spectrum (but not continuum-normalized).

Originally, the plan was to obtain spectra of 9 targets (Table 1), but actually we successfully extracted spectra of 20 NIR sources, because other stars fell inside the slit together with the program sources. Some of them are also hot stars belonging to the associated stellar clusters, but a significant fraction of the "extra" sources are late-type field stars.

All spectra have been classified in three groups. In the first one, the detected lines are characteristic of hot stars ( $\text{Br}\gamma$ ,  $\text{HeI } 2.058 \mu\text{m}$ ,  $\text{HeI } 2.113 \mu\text{m}$ ,  $\text{HeII } 2.185 \mu\text{m}$ ,  $\text{CIV } 2.078 \mu\text{m}$ ,  $\text{NIII } 2.116 \mu\text{m}$ , among others.); they are shown in Figure 3 in order of increasing  $\text{Br}\gamma$  equivalent width (EW). An unexpected spectrum was obtained for IRAS15408-5356\_IRS3a and IRAS16132-5039\_IRS3. They show the hydrogen  $\text{Br}\gamma$  and the  $\text{HeI}$  lines typical of hot stars, but also CO band-head overtone lines in absorption, characteristic of late-type stellar atmospheres. The implications of these findings will be discussed in Section 4. The spectra of the sources in the second group, shown in Figure 4, present metallic lines (Na, Ca, Mg, etc.) and molecular lines (CO overtones), as expected in late-type star spectra. The third group shows H and He in emission but no photospheric absorption lines, which is characteristic of young stellar objects (YSOs); their spectra are shown in Figure 5.

### 3.2. Spectral classification

The library of  $K$ -band early-type spectra compiled by Hanson, Conti & Rieke (1996) was used to classify the stars in our sample. Since both spec-

tra have similar resolution, the classification of the stars in group 1 was made by direct comparison. For each star, we show the library spectrum that best matches the target, as well as an earlier and a later spectral type library spectrum (Figures 6-9); the spectral types obtained are presented in column 4 of Table 2.

The absolute  $M_J$  magnitudes (column 5 of Table 2) were obtained using the intrinsic colors given by Koornneef (1983), transformed into the 2MASS photometric system, because the photometric data used in our work were calibrated using 2MASS photometry; the  $M_V$  magnitudes were obtained from Hanson et al. (1997) for main sequence star and Walborn (2002) for O3/O4Iaf\* stars. Columns 6 and 7 list the intrinsic  $(J - H)_0$  and  $(H - K)_0$  colors corresponding to each spectral type. Columns 8, 9, 10 and 11 list the measured  $J$  and  $K$  magnitudes, as well as the  $(J - H)$  and  $(H - K)$  colors obtained from previous works (Roman-Lopes et al. 2003, Roman-Lopes & Abraham 2004a, 2004b, Ortiz et al. 2007).

### 3.3. Determination of the distances

The distances  $d$  to the stars were determined using absolute and measured magnitudes presented in Table 2, in the equation:

$$m_\lambda - M_\lambda = 5 \log[d(\text{pc})] - 5 + A(\lambda) \quad (1)$$

The absorption  $A(\lambda)$  is related to the color excess  $E(J - H)$  and  $E(H - K)$  through the functions  $F_J(R) = A(J)/E(J - H)$  and  $F_K(R) = A(K)/E(H - K)$  that depend on the ratio of the total to selective extinction  $R = A_V/E(B - V)$ . Using the interstellar extinction laws given by Fitzpatrick (1999), it is possible to obtain the ratios  $A_J/A_V = f_J(R)$ ,  $A_K/A_V = f_K(R)$  and  $E(J - H)/E(B - V) = g_J(R)$ ,  $E(H - K)/E(B - V) = g_K(R)$  from which the functions  $F(R) = Rf(R)/g(R)$  can be derived.

A source of uncertainty in the determination of the distance originates from the use of standard interstellar extinction law, which it is represented by  $R = 3.1$ , though it is common to find  $R$  in the range  $2.8 - 5.8$  along the galactic plane (Johnson 1965, Tapia 1981, Fitzpatrick 1999, Indebetouw et al. 2005, Nishiyama et al. 2006). This effect is probably produced by differences in metallic-

TABLE 2  
DERIVED SPECTRAL TYPES FOR THE HOT STARS IN OUR SAMPLE

Source (1)	$\alpha$ (J2000) (2)	$\delta$ (J2000) (3)	S.T. (4)	$M_J$ (5)	$(J-H)_o$ (6)	$(H-K)_o$ (7)	$J$ (8)	$(J-H)$ (9)	$K$ (10)	$(H-K)$ (11)
IRAS09149-4743_IRS1a	09h16m43.50s	-47°56'23.0"	B0V	-2.21	-0.16	-0.01	10.70	0.80	9.40	0.50
IRAS09149-4743_IRS2	09h16m47.94s	-47°57'18.0"	O9V	-3.00	-0.18	-0.01	9.72	0.66	8.68	0.38
IRAS09149-4743_IRS31	09h16m47.77s	-47°57'15.1"	B7/B8V	-0.27/0.29	-0.07	+0.02	13.34	0.80	12.25	0.29
IRAS15408-5356_IRS1	15h44m43.40s	-54°05'53.7"	O5.5V	-4.05	-0.20	-0.01	10.76	1.37	8.57	0.82
IRAS15408-5356_IRS3a	15h44m56.17s	-54°07'18.1"	O9.5V	-2.85	-0.16	-0.01	11.25	1.17	9.50	0.58
IRAS15408-5356_IRS3b <sup>1</sup>	15h44m56.17s	-54°07'18.1"	B3/B5V	-0.45/+0.15	-0.11	+0.01	—	—	12.0	—
IRAS16132-5039_IRS3	16h16m56.01s	-50°47'22.7"	O9.5/B0V	-2.85/-2.21	-0.18/-0.16	-0.01	11.77	0.76	10.30	0.71
IRAS16132-5039_IRS3_ap3	16h16m50.84s	-50°47'44.2"	B8/B9V	-0.27/0.29	-0.03	-0.01	12.71	0.15	12.50	0.06
IRAS16177-5018_IRS1	16h21m31.60s	-50°25'08.3"	O4If*	-6.85	-0.21	-0.01	16.65	3.92	10.21	2.52

<sup>1</sup>No  $J$  and  $H$  photometry available

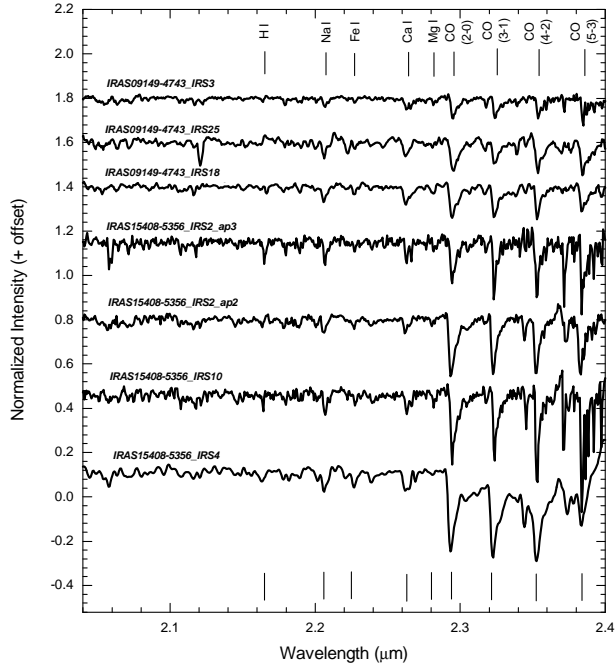


Fig. 4.— GNIRS spectra of the late-type stars. All spectra were continuum flux normalized and are at same scale.

ity and grain size distribution (Savage & Mathis 1979). It was taken into account by using  $R = 2.8$ , 3.1 and 5.0, and the distance to each star (column 12) was calculated as the average of these individual values.

Another important source of error results from the spectral type determination itself, which has an uncertainty of about  $\pm$  one sub-type. For O-type stars it represents about 0.2 magnitudes in the NIR, whereas for early-B stars it is about 0.6 magnitude (Hanson et al. 1997).

A third source of uncertainty results from the fact that the stars can be surrounded by disk and/or dust cocoons, which produce excess emission in the NIR (Grasdalen et al. 1975, Glass 1979, Lada & Adams 1992), especially in the  $K$ -band. In order to minimize this effect, we used both the  $J$  and  $K$  band to derive the distances.

Table 3 shows the values of  $E(J - H)$  (Column 2) and  $E(H - K)$  (Column 7);  $A_J$  (Columns 3, 4 and 5) and  $A_K$  (Columns 8, 9 and 10) obtained assuming ratios of total to selective extinction of 2.8, 3.1 and 5.0, and the stellar distances  $d$  (column 12). The quoted errors for the distances are the standard deviation of the averaged distance, which include the errors associated to the photometry, interstellar extinction law, and spectral type, as discussed above. Finally, the distance to each cluster (Column 13) was computed as the average of the distances to the stars in each cluster; the total error of these values is the square root of the sum in quadrature of the individual errors.



TABLE 3  
SUMMARY OF THE EXTINCTION VALUES AND DISTANCES TO THE PROGRAM STARS

Source	$E(J - H)$	$A_J$ $R = 2.8$	$A_J$ $R = 3.1$	$A_J$ $R = 5.0$	$A_V$ $R = 3.1$	$E(H - K)$	$A_K$ $R = 2.8$	$A_K$ $R = 3.1$	$A_K$ $R = 5.0$	$A_V$ $R = 3.1$	$d_{\text{aver}}^1$ (kpc)	$d_{\text{cluster}}^2$ (kpc)
(1)	(2)	(3)	(4)	(5)	(6)	(7)	(8)	(9)	(10)	(11)	(12)	(13)
IRAS09149-4743_IRS1a <sup>3</sup>	0.96	2.5	2.6	2.8	9.1	0.51	1.0	1.0	1.1	8.9	$1.20 \pm 0.12$	$1.3 \pm 0.2$
IRAS09149-4743_IRS2	0.84	2.2	2.3	2.5	8.0	0.39	0.9	0.9	1.0	6.8	$1.27 \pm 0.13$	
IRAS09149-4743_IRS31	0.87	2.3	2.3	2.6	8.3	0.27	0.9	0.9	1.0	4.7	$1.37 \pm 0.19$	
IRAS15408-5356_IRS1	1.57	4.1	4.2	4.6	14.9	0.83	1.6	1.7	1.9	14.4	$1.34 \pm 0.16$	$1.3 \pm 0.2$
IRAS15408-5356_IRS3a	1.33	3.5	3.6	3.9	12.6	0.59	1.4	1.4	1.6	10.2	$1.32 \pm 0.20$	
IRAS15408-5356_IRS3b <sup>4</sup>	*	*	*	*	12.6	*	*	*	*	10.2	$1.24 \pm 0.21$	
IRAS16132-5039_IRS3 <sup>3</sup>	0.92	2.4	2.5	2.7	8.7	0.72	1.0	1.0	1.1	12.5	$2.15 \pm 0.50$	$2.3 \pm 0.4$
IRAS16132-5039_3(ap3)	0.22	0.6	0.6	0.7	2.1	0.04	0.2	0.2	0.3	0.7	$2.64 \pm 0.30$	
IRAS16177-5018_IRS1 <sup>3</sup>	4.13	10.7	11.1	12.1	39.2	2.53	4.3	4.5	4.9	43.9	$2.58 \pm 0.68$	$2.6 \pm 0.7$

<sup>1</sup>The distances to the individual stars represent the average of the values obtained using the three absorption laws ( $R = 2.8, 3.1$  and  $5.0$ )

<sup>2</sup>The distance to each cluster represents the average value of the individual stellar distances

<sup>3</sup>According to the previous NIR studies, this source presents some excess emission in the  $K$ band. For details, see the references in the text.

<sup>4</sup>The extinction for this source has been assumed to be the same as for IRS3a. See text for details.

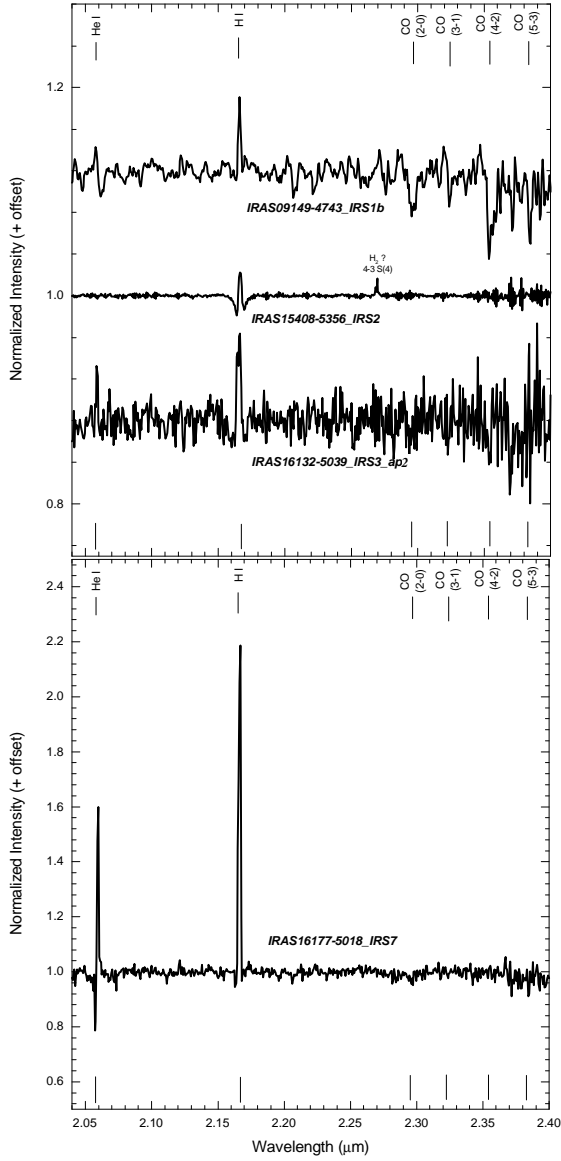


Fig. 5.— GNIRS spectra of massive YSO's in our sample. All spectra were continuum flux normalized and are at the same scale.

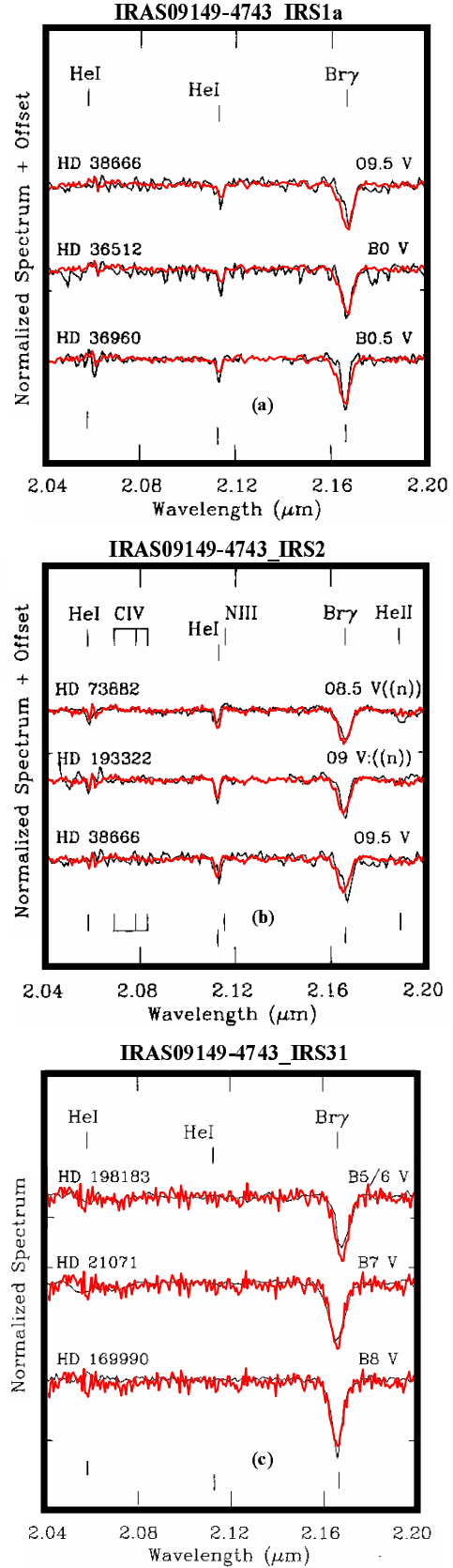


Fig. 6.— GNIRS spectra of IRAS09149-4743 sources (red line) overlaid on *K*-band spectra (black lines) from the library of Hanson et al.

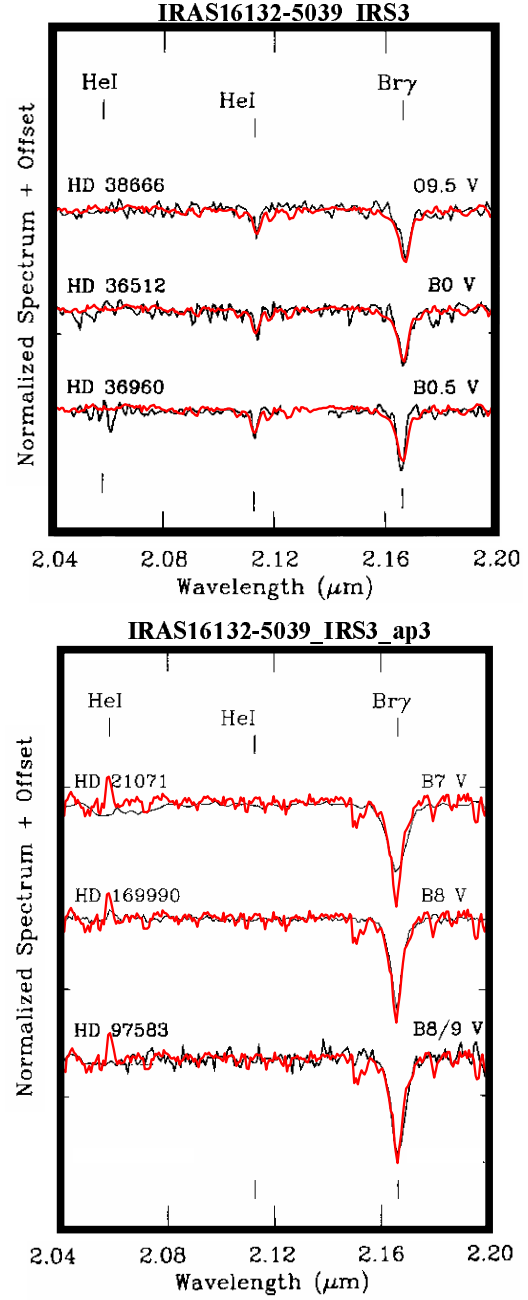
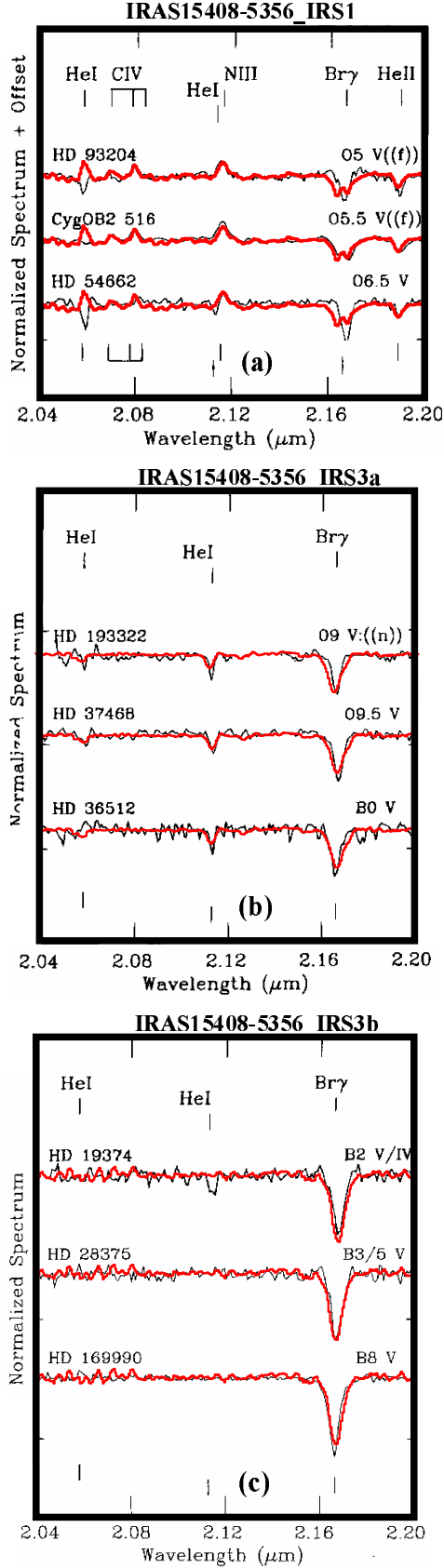


Fig. 8.— GNIRS *K* band spectra (red lines) of sources in the cluster associated to the IRAS16132-5039 source, overlaid on *K* band spectra (black lines) from the library of Hanson et al. (1996).

Fig. 7.— GNIRS spectra of IRAS15408-5356 IRS1, IRS3a and IRS3b sources (red lines) overlaid on *K* band spectra (black lines) from the

## 4. Discussion

The physical parameters of the stars surveyed in this work were calculated from their classification based on spectral features in the  $K$ -band. Although Bik et al. (2005) pointed out that this classification may not be as reliable as that based in the visual spectrum, this tool probably represents the best method to determine spectral types of stars still embedded in the parental molecular cloud, especially when the extinction limits the observation to near-infrared wavelengths.  $K$ -band spectroscopy has been used by other authors to study young, massive stellar candidates, chosen according to their IRAS color indices (Martín-Hernández et al. 2003, Bik et al. 2005, 2006). Some of the sources in this work have been observed during previous surveys. In this section, we carry out a discussion on the main results obtained in this work, as well as a comparison with previous results obtained by other authors.

### 4.1. The IRAS09149-4743 cluster

In this region, three program stars were chosen for observation: IRS1, IRS2 and IRS3. In addition to that, three other sources located nearby had their spectra taken as well: IRS18, IRS25, and IRS31. Their relative positions are shown in Fig. 1. The source labeled as IRS1 in Ortiz et al. (2007) has been resolved into two stars in this work: IRS1a and IRS1b (see the inset in Fig. 1a). The spectra of IRS1a and IRS2, shown in Fig. 3, exhibit two important diagnostic lines commonly found in stars earlier than B1V: H $\gamma$  Br- $\gamma$  at  $2.166\mu\text{m}$  and the HeI line at  $2.113\mu\text{m}$ . The source IRS1a has been classified as a B0V star (Figure 6a), affected by 9 magnitudes of visual extinction (Table 3), which places it at a distance of about  $1.20 \pm 0.12$  kpc. IRS2, belonging to the nearby sub-cluster located 1.1 arcmin to the southeast of IRS1 (Ortiz et al. 2007), is an O9V star (Figure 6b), affected by an interstellar absorption of 7–8 visual magnitudes, placed at virtually the same distance as IRS1a ( $1.27 \pm 0.13$  kpc).

In Figure 5 we can see that IRS1b shows no photospheric spectral lines, but Br $\gamma$  in emission and some CO overtone band-heads in absorption, characteristic of YSO's (Casali & Eiroa 1996, Hoffmeister et al. 2006). These CO lines are believed to be formed in a warm and dense circumstellar

shell, possibly a relic of a former accretion disk. The physical reason for the existence of CO in absorption or emission is related to the disk opacity, which in turn depends on the mass accretion rate, as shown in Calvet et al. (1991). Ortiz et al. (2007) also point out that IRS1a+b shows intense infrared emission beyond  $5\mu\text{m}$ , usually attributed to warm dust. Based on the present data, we can now state that the observed infrared excess comes from IRS1b, the nearby companion of the IRS1a source.

IRS31 is a member of the small sub-cluster which contains also the main ionizing source of the HII region, IRS2. The spectrum of IRS31 shown in Fig. 3 exhibits a strong Br- $\gamma$  line, characteristic of late-B and early-A stars. This star has been classified as B7V-B8V (Figure 6c), absorbed by 5–8 visual magnitudes, which implies that its distance is  $1.37 \pm 0.19$  kpc.

IRS3 is a highly reddened IR source (Ortiz et al. 2007), located at about 1 arcmin west of IRS1 (Figure 1a). Its spectrum, shown in Figure 4, exhibits metallic and molecular absorption lines, such as the CO (2,0) and (3,1) transitions at 2.29 and  $2.32\mu\text{m}$  respectively, as well as the CaI and NaI lines at 2.21 and  $2.26\mu\text{m}$ , typical of late-type stars. Ortiz et al. (2007) previously suggested that this star might be a background late-type giant. Its position in the  $(J-H)$  versus  $(H-K)$  diagram is within the normal reddening band, and its spectrum shows features commonly seen in K and M stars. Thus, assuming its spectral classification as early-K, one can estimate a lower limit for its distance. In this case, its absolute magnitude and intrinsic colour index would be  $M_J = -1.9$  and  $(J-H) = 0.62$ , which implies a colour excess of  $E(J-H) = 1.42$ . If one assumes  $R = 3.1$  then  $A_J = 4.34$  and  $d = 2.5$  kpc. On the other hand, if  $R = 5.0$ ,  $A_J = 4.76$ , and  $d = 2.0$  kpc. In any case, the distance to this star would be twice as large as the distance to RCW 41. Besides IRS3, two other stars in the neighbourhood have been classified as late-type: IRS18 and IRS25 (Fig. 4). Similarly to IRS3, they occupy a position in the  $(J-H)$  versus  $(H-K)$  C-C diagram within the band of severely reddened giant stars, consistent with their classification as late-type stars, and their  $JHK$  magnitudes given in Ortiz et al. (2007) imply that they must also be background objects.

It can be seen that the distances to all the mas-

sive stars in this region are similar, which gives a mean distance of  $1.3 \pm 0.2$  kpc for the cluster. This value can be compared with the photometric distance of  $0.7 \pm 0.2$  kpc quoted by Liseau et al. (1992) for cloud A in the VMR complex, and the kinematic distance of 1 kpc inferred from CO observations by Murphy & May (1991). Considering the complexity of the VMR and the small radial velocity resulting from its position close to  $l = 270^\circ$ , the previous measurements are consistent with our determination.

#### 4.2. The IRAS15408-5356 cluster

In this cluster, spectra of four program stars (IRS1, IRS2, IRS3, and IRS4) have been obtained. The spectrum of IRS1 is shown in Figure 3. It presents features typical of very hot stars, such as C IV (at  $2.078\mu\text{m}$ ) and N III (at  $2.116\mu\text{m}$ ) in emission, characteristic of stars with spectral type earlier than O6v (Hanson et al. 1996). A direct comparison with the library templates of Hanson et al. (1996) allowed us to classify it as O5.5v (Figure 7a). Since Morisset (2004) argued that the relative intensities of mid-infrared emission lines observed by the *Infrared Space Observatory* (ISO) require an ionizing source with effective temperature  $T_{\text{eff}} = 48,700\text{K}$ , equivalent to an O3v star, we conclude that other stars must also contribute to the total ionizing luminosity.

The spectrum of IRS2, seen in Figure 5, does not present any evident photospheric feature, except for the Br $\gamma$  emission line, superposed on an absorption profile. Another emission line near  $2.27\mu\text{m}$  might be due to the 4-3 S(4) H $_2$  transition. Differently from IRAS 09149-4743 IRS1b, the spectrum of IRS2 does not show any evidence of a CO environment that could be associated with circumstellar disks. However, since this object shows large IR color excess (Roman-Lopes & Abraham 2004b) and is associated with the bright source MSX6C-G326.6570+00.5912, we classified it as an YSO.

Three additional less luminous stars located near IRS2 fell into the slit: IRS10 and other two sources not included in the previous photometric study of the region, labeled IRS2\_ap2 and IRS2\_ap3. Their spectra, shown in Figure 4, are characteristic of late-type stars. This result implies that IRS10 is not one of the ionizing sources of RCW95, as previously proposed considering

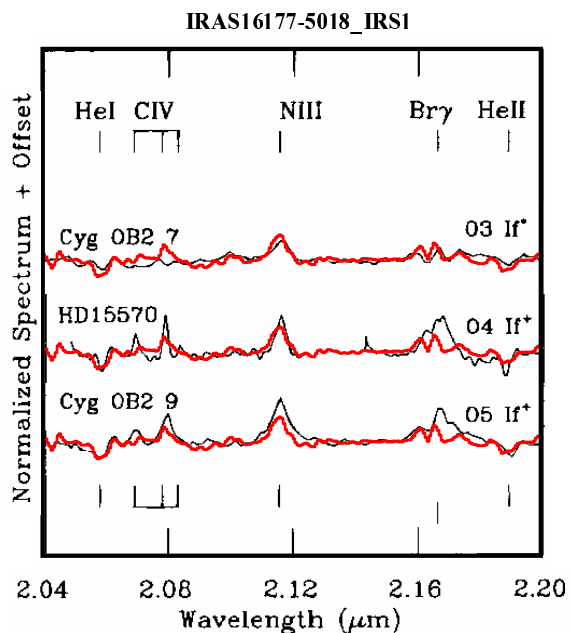


Fig. 9.— GNIRS spectrum of the IRAS16177-5018-IRS1 source (light gray lines). The spectrum can be compared with those of O3-O5If\* stars taken from the library of Hanson et al. 1996 (black). All spectra have been flux normalized and are set at same scale.

its *JHK* magnitudes and colors (Roman-Lopes & Abraham 2004b). Their location in the C-C diagram seems to result from their low effective temperatures and the high extinction of the cloud, which together mimic the color indices of young, massive stars.

IRS3 was previously suggested as one of the main ionizing sources of RCW 95, together with IRS1. This object actually consists of at least two stars, labeled IRS3a and IRS3b, as shown in the inset in Figure 1b. IRS3a presents an unexpected spectrum; it does show the hydrogen Br $\gamma$  and the HeI lines typical of hot stars, as well as CO band-head overtone lines in absorption, characteristic of late-type stellar atmospheres. Although CO overtone bands in absorption have been widely reported in low-mass YSO spectra (Straw, Hyland & Mc Gregor 1987, Straw et al. 1987, Carr 1989, Casali & Matthews 1992), it has also been found in a few early-B stars (Hoffmeister et al. 2006). The origin of these CO features is not clear, it might be the signature of a cold star in the same line of sight or simply neutral gas in the interface between the HII region and the molecular cloud. Apart from the CO lines beyond  $2.3\ \mu\text{m}$ , this star can be classified as O9.5v, as presented in Figures 7b. IRS3b has been classified as an B3/B5v star, as shown in Figure 7c.

The spectrum of IRS4, shown in Figure 4, is clearly late-type, with strong CO absorption lines in the spectral region between  $2.29\ \mu\text{m} < \lambda < 2.4\ \mu\text{m}$ . One can see also a few metallic lines, probably due to NaI and CaI transitions, which reinforces this classification.

The distances to the early-type sources have been determined from their spectral types, *J* and *K* magnitudes, and  $E(J-H)$  and  $E(H-K)$  color excesses, as described in Section 3.3, and presented in Table 3. Since no photometric data are available for IRS3b, we used the visual absorption calculated for IRS3a instead, and the *K* magnitude obtained from the GNIRS *K*-band acquisition image. The instrumental GNIRS magnitudes were calibrated using the combined *K* magnitudes of IRS3a and IRS3b, obtained from the work of Roman-Lopes & Abraham (2004b). The resulting individual *K* magnitudes are 9.5 and 12.0 for IRS3a and IRS3b, respectively.

Bik et al. (2005) obtained high-resolution *K*-band spectra of two stars in common with the

present work: 15408nr1410 and 15408nr1454, and classified them as O5v-O6.5v and O8v-B2.5v, respectively. According to their coordinates (Bik 2004), they correspond to the sources named in this work as IRS1 and IRS3a, classified as O5.5v and O9.5v, respectively, in agreement with their work. Despite the higher resolution in Bik et al. (2005), the spectral types determined in our work are in a narrower range, which implies in more precise distance determination.

The derived distances to all stars observed in this cluster are similar, like in IRAS09149-4743, ranging from  $1.32 \pm 0.20$  kpc for IRS3a to  $1.34 \pm 0.16$  kpc for IRS1, giving a mean distance of  $1.3 \pm 0.2$  kpc for the IRAS15408-5356 cluster. This is half of what was derived from the Galactic rotation curve (2.4 kpc) by Givon et al. (2002), assuming a galactocentric distance of 8.5 kpc and a solar rotation velocity of  $220\ \text{km s}^{-1}$ . Large differences between the kinematic distances, derived from radio observations and those obtained by spectroscopic parallaxes were also found by Blum et al. (1999, 2000) and Figuerêdo et al. (2005), showing the importance of spectroscopic parallaxes for a better understanding of the rotation curve of our galaxy.

#### 4.3. The clusters in the RCW106 region

The two clusters associated to IRAS16132-5039 and IRAS16177-5018 are part of the RCW106 HII complex. Only one program star was observed in each cluster: IRS3 in the former cluster and IRS1 in the latter.

During the observation of the IRAS16132-5039 IRS3 three stars fell into the spectrograph slit: IRS3 itself, which has been classified as O9.5V/B0V (Figure 8a), and two additional sources: IRS3\_ap2, identified as an YSO (Figure 5), and IRS3\_ap3, probably a B8V/B9V star (Figure 8b). Similarly to IRAS15408-5356 IRS3a, the spectrum of IRAS16132-5039 IRS3 presents H and He lines as well as CO overtone lines, their possible origin was already discussed in the previous section

In the observation of IRAS16177-5018 cluster, two stars fell into the slit: the program star IRS1, and IRS7, as designated in Roman-Lopes et al. (2003). The spectrum of IRS1 shows C IV, N V, and N III emission lines at  $2.078\ \mu\text{m}$ ,  $2.100\ \mu\text{m}$ , and

2.116  $\mu\text{m}$ , respectively, HeII at 2.189  $\mu\text{m}$  in absorption, and absent Br $\gamma$  line. Figure 9 shows that these characteristics correspond to an O4 If<sup>+</sup> supergiant star. The spectrum of this star, designated as 16177nr405, was also obtained by Bik et al. (2005); it shows CIV, NIII, Br $\gamma$  and HeI in emission, the first two were used to classify the star as O5V–O6.5V, the last two were considered "nebular". In our work, the classification was based also on the Br $\gamma$  and HeI lines, which were probably more properly subtracted from the nebular contribution. The presence of a supergiant star could be questioned in view of the early evolutionary stage of the cluster. However, other O-type supergiants have been previously found in stellar clusters with ages ranging from 0.5 to 1.9 Myr (Massey et al. 2001).

The spectrum of IRS7 shows several characteristics of an YSO, as it can be seen in Figure 5. A prominent P-Cygni profile of the HeI line at 2.058  $\mu\text{m}$  and the CO overtone band head at 2.295  $\mu\text{m}$  strongly suggest the existence of circumstellar material around an early-type star. Similarly to IRAS 09149-4743IRS1b, the CO features probably result from the presence of a high-density, warm circumstellar disk. As pointed out by Roman-Lopes et al. (2003) this object coincides with the mid-infrared source MSX6C-G333.3072-00.3666, which reinforces its classification as an YSO.

The distances to IRS3, IRS3\_ap3 and IRS1 were found to be  $2.15 \pm 0.50$ ,  $2.64 \pm 0.30$  and  $2.58 \pm 0.68$  kpc, respectively (Table 3). Therefore, it can be concluded that both clusters are located at the same distance. The kinematic distance to RCW 106 was determined by Caswell & Haynes (1985) as 3.8 kpc, assuming galactocentric distance  $R_0 = 10$  kpc and solar rotational velocity of  $\Theta_\odot = 250 \text{ km s}^{-1}$ . However, if one assumes  $R_0 = 8.5$  kpc and  $\Theta_\odot = 220 \text{ km s}^{-1}$  (Honma & Sofue 1997), modifying the rotation curve of Rohlfs & Kreitschmann (1987) to these values, the kinematic distance would drop to 3.2 kpc. Considering the uncertainties of both methods, this value is compatible with the spectroscopic distances obtained in this work. The distance to this cluster obtained by Bik et al. (2005) is in the range 1.0–3.7 kpc, because of their coarser spectral classification, but it is consistent with our results.

## 5. Conclusions

GNIRS *K*-band spectroscopic observations of stars belonging to highly reddened southern hemisphere young stellar clusters are reported. All the GNIRS program targets (associated with the sources IRAS09149-4743, IRAS15408-5356, IRAS16132-5039 and IRAS16177-5018), but one of them (IRAS15408-5356IRS4) present spectral characteristics of massive stars and/or YSOs, as inferred from previous NIR imaging surveys.

By comparing the GNIRS *K*-band spectra of the program stars with those in the *K*-band library of OB stars made by Hanson et al. (1996), it was possible to derive spectral type classification of the most prominent sources in each cluster. Although the spectral types determined in this work may differ from previous classifications based on photometric data alone, the present results confirm the majority of the candidates suggested in previous works as the main ionizing sources of the surveyed HII regions.

Using the *JHK* photometry obtained from previous surveys and the results of Fitzpatrick (1999), we derived values for the extinctions and distances to the clusters. We found that the distances to the clusters belonging to the Vela Molecular Ridge and the RCW106 complex agree with previous results obtained from IR and radio studies. The only exception is the RCW 95 complex, which spectroscopic distance was half the value derived from the galactic rotation curve.

## Acknowledgments

This work was partially supported by the Brazilian agencies CNPq and FAPESP. A. Roman-Lopes thanks financial support from FAPESP under the program 04/10375-2. A.R.-A. acknowledges support from the Brazilian Agency CNPq under program 311476/2006-6. Based on observations obtained at the Gemini Observatory, which is operated by the Association of Universities for Research in Astronomy, Inc., under a cooperative agreement with the NSF on behalf of the Gemini partnership: the National Science Foundation (United States), the Science and Technology Facilities Council (United Kingdom), the National Research Council (Canada), CONICYT (Chile), the Australian Research Council (Australia), Ministério da Ciência e Tecnologia (Brazil) and SE-

CYT (Argentina).

## REFERENCES

- Arias, J., Barba, R., Morrell, N., MNRAS, 2007, 374, 1253
- Balog, Z., Kenyon, S., Lada, E., Barsony, M., 2004, AJ, 128, 2942
- Barba, R. & Arias, J., A&A, 2007, 471, 841
- Bik, A., 2004, The stellar content of high-mass star-forming regions, PhD Thesis, University of Amsterdam, The Netherlands.
- Bik, A. & Thi, W.F., 2004, A&A, 427, L13
- Bik, A., Kaper, L., Hanson, M.M. & Smits, M., 2005, A&A, 440, 121
- Bik, A., Kaper, L. & Waters, L.B.F.M., 2006, A&A, 455, 561
- Blum, R. D., Damineli, A., Conti, P. S., 1999, AJ, 117, 1392
- Blum, R. D., Conti, P. S., Damineli, A. 2000, AJ, 119, 1860
- Borissova, J.; Ivanov, V. D.; Minniti, D.; Geisler, D.; Stephens, A. W., 2003, A&A, 411, 83
- Bronfman L., Nyman L.-A., May J., 1996, A&A 115, 81
- Calvet, N., Patiño, A., Magris, C. G., D'Alessio, P., 1991, ApJ, 380, 617
- Carr, John S., 1989, ApJ, 345, 522
- Casali, M., Matthews, H., 1992, MNRAS, 258, 399
- Casali, M. M., Eiroa, C., 1996, A&A, 306, 427
- Caswell J.L., Haynes R.F., 1987, A&A, 171, 261
- Dutra C.M., Bica E., Soares J., & Barbuy B., 2003, A&A, 400, 533
- Elias, J. H., Joyce, R. R., Liang, M., Muller, G. P., Hileman, E. A., & George, J. R., in Ground-based and Airborne Instrumentation for Astronomy, eds. I. S. McLean and I. Masanori, 2006, SPIE, 6269, 138.
- Figuerêdo, E., Blum, R. D., Damineli, A., Conti, P. S., 2002, AJ, 124, 2739
- Figuerêdo, E., Blum, R. D., Damineli, A., Conti, P. S., 2005, AJ, 129, 900
- Fitzpatrick E.L., 1999, PASP, 111, 63
- Giveon A., Sternberg A., Lutz D., Fruchtgruber H. & Pauldrach A.W.A., 2002, ApJ, 566, 880
- Glass I.S., 1979, MNRAS, 187, 305
- Gomes, M., Kenyon, S., 2001, AJ, 121, 974
- Grasdalen G., Joyce R., Knacke R.F., Strom S.E. & Strom K.M., 1975, AJ, 80, 117
- Hanson, M.M., Conti, P.S. & Rieke, M.J., 1996, ApJS, 107, 281
- Hanson M.M., Howarth I.D. & Conti P.S., 1997, ApJ, 489, 698
- Hanson M.M., Luhman K., Rieke, G., 2002, ApJS, 138, 35
- Hanson M.M., Kudritzki, R.-P.; Kenworthy, M. A.; Puls, J.; Tokunaga, A. T., 2005, ApJS, 161, 154
- Hoffmeister, V., Chini, R., Scheyda, C., Nurnberger, D., Vogt, N., Nielbock, N., 2006, A&A, 457, L29
- Honma M. & Sofue Y., 1997, PASJ, 49, 453
- Horner, D., Lada, E., Lada, C., 1997, AJ, 113, 1788
- Indebetouw, R., Mathis, J. S., Babler, B. L., Meade, M. R., Watson, C., Whitney, B. A., Wolff, M. J., Wolfire, M. G., Cohen, M., Bania, T. M., and 10 coauthors, 2005, ApJ, 619, 931
- Johnson, H.L, 1965, ApJ, 141, 923
- Koornneef, J., 1983, A&A, 128, 84
- Kumar, M., Kamath, U. & Davis, C., 2004, MNRAS, 353, 1025
- Lada, C., Adams, F., 1992, ApJ, 393, 278
- Lada, C., Muench, A., 2004, AJ, 128, 1254
- Leistra, A.; Cotera, A. S.; Liebert, J.; Burton, M., 2005, AJ, 130, 1719



- Liseau R., Lorenzetti D., Nisini B., Spinoglio L. & Moneti A., 1992, A&A, 265, 577
- Martín-Hernández, N.L., Bik, A., Kaper, L., Tielens, A.G.G.M. & Hanson, M.M., 2003, A&A, 405, 175
- Massey, P., DeGioia-Eastwood, K., Waterhouse, E., 2001, AJ, 121, 1050
- Massi, F., Lorenzetti, D., Giannini, T., 2003, A&A, 399, 147
- Morisset, C., 2004, ApJ, 601, 858
- Nishiyama, S., Nagata, T., Kusakabe, N., Matsumaga, N., Naoi, T., Kato, D., Nagashima, C., Sugitani, K., Tamura, M., Tanab, T., Sato, S., 2006, ApJ, 638, 839
- Ortiz R., Roman-Lopes A. & Abraham Z., 2007, A&A, 461, 949
- Rieke, G.H. & Lebofsky, M.J., 1985, ApJ, 288, 618
- Rodgers A.W., Campbell C.T. & Whiteoak J.B., 1960, MNRAS, 121, 103
- Rohlfs K. & Kreitschmann J., 1987, A&A, 178, 95
- Roman-Lopes A., Abraham Z. & Lépine J.R.D., 2003, AJ, 126, 1896
- Roman-Lopes A. & Abraham Z., 2004a, AJ, 127, 2817
- Roman-Lopes A. & Abraham Z., 2004b, AJ, 128, 2364
- Roman-Lopes A. & Abraham Z., 2006a, AJ, 131, 951
- Roman-Lopes A. & Abraham Z., 2006b, AJ, 131, 2223
- Roman-Lopes A., 2007, A&A, 471, 813
- Savage, B.D. & Mathis, J.S., 1979, ARA&A, 17, 73
- Simpson J.P. & Rubin R.H., 1990, ApJ, 354, 165
- Straw, S. M., Hyland, A. R., McGregor, P. J., 1987, ApJs, 69, 99
- Straw, S., Hyland, A. R., Jones, Terry J., Harvey, Paul M., Wilking, Bruce A., Joy, M., 1987, ApJ, 314, 283
- Tapia M., 1981, MNRAS, 197, 949
- Walborn, N.R., 2002, AJ, 124, 507
- Whitney, B., Indebetouw, R., Babler, B., and 19 co-authors, 2004, ApJS, 154, 315
- Wood D.O.S. & Churchwell E., 1989, ApJ, 340, 265